Article

Not peer-reviewed version

Corallopyronin B Antibiotic Construct from Heterogeneous Soil Environments in Egypt

Mohammed MahmoudShawky Kassab *

Posted Date: 13 May 2024

doi: 10.20944/preprints202405.0769.v1

Keywords: Corallopyronin B; Infection; Antimicrobial; Resistance; Myxobacteria

Article

Corallopyronin B Antibiotic Construct from Heterogeneous Soil Environments in Egypt

Mohammed Kassab

Professor of Microbiology and Immunology, Department of Microbiology and Immunology, Faculty of Pharmacy, Cairo University, Egypt; ksabmhmd676@gmail.com; Tel.: +201032579044

Abstract: Background: Antibiotic resistance is an urgent issue everywhere in the globe. It is necessary to look into new sources of antibiotics to address this issue. Methodology: Several soil conditions in Egypt were examined to create bacterial isolates that generated the antibiotic chemical *Corallopyronin B*. Using *reversed-phase HPLC*, *Myxopyronin B* was purified. The test antibiotic's minimum inhibitory concentration (*MIC*) and in vitro antibacterial activity were ascertained using *the paper disc diffusion assay* and *the broth microdilution technique*. Furthermore, in *stages 1/2 of randomized clinical trials including human and animal models*, pharmacokinetics, adverse drug reactions, and the in vivo antibacterial spectrum were discovered. Results**:** The soil bacterial isolate *Corallococcus coralloides DSM 2259*, which was grown on *a Casein yeast peptone* (*CYP*) *plate*, produced *Corallopyronin B* from its culture supernatant. At *MICs* more than *100 mcg/ml*, the test antibiotic inhibited the growth of many *Gram -ve* bacteria, including *Escherichia coli*, while also preventing the growth of numerous *Gram +ve* bacteria, with *MICs* ranging from *1 to 10 mcg/m*l. Eukaryotic cells, on the other hand, including those in humans and fungi, were unharmed. Conclusion: The current work was noteworthy since it involved the production of the bactericidal antibiotic *Corallopyronin B* from *Corallococcus coralloides DSM 2259* which was isolated from several soil environments in Egypt.

Keywords: Corallopyronin B; infection; antimicrobial; resistance; myxobacteria

1. Introduction

Selective toxicity is a requirement for an antibiotic's medicinal value [1]. Compared to human cells, the activity of bacteria must be greatly inhibited [2]. Since antibiotic resistance is a significant, worldwide difficulty that needs to be addressed, the hunt for new sources of antibiotics is crucial [3]. Antibacterial medications primarily target four structures: nucleic acids, cell membranes, ribosomes, and cell walls [4]. Due to their lack of a cell wall and the presence of special ribosomes, nucleic acid enzymes, and sterols in their membranes, these medications do not affect human cells [5]. Antibiotics that are classified as bactericidal are expeditious in killing bacteria [6]. Contrarily, bacteriostatic medications stop the development of microorganisms [7]. The patient's phagocytes eradicate the infection while using bacteriostatic medications [8].

Bacteriocidal medications have to be administered to patients with low neutrophil levels [9]. *Corallopyronins* are a class of alpha-pyrone antibiotics [10]. A family of heterocyclic chemical compounds is known as pyrones [11]. They feature a ketone functional group and an unsaturated six-membered ring with one oxygen atom [12]. The terms *4-pyrone* and *2-pyrone* refer to the two isomers [13]. Because Corallopyronins do not cross-resistance with any other medicine, they may be able to help solve the developing issue of drug resistance in *TB* [14]. *Methicillin-resistant Staphylococcus aureus* (*MRSA*) therapy could potentially be advantageous [15]. The cognitive content of the current study was to evaluate the synthesis of a new antibiotic named *Corallopyronin B* under diverse soil conditions in Egypt. In *phase 1/2 randomized clinical trials involving humans*, antibacterial activity was also examined.

 doi:10.20944/preprints202405.0769.v1

2. Patients and Methods

2.1. Ethical Statement

All relevant institutional, national, and/ or worldwide standards on the use and care of humans and animals were given priority in the current study. The Ethical Committee for Human and Animal Handling at Cairo University (*ECAHCU*), housed at the Faculty of Pharmacy, Cairo University, Egypt, approved all study procedures involving humans and animals per the recommendations of the Weatherall Report (approval number *T716-2022*). The number and degree of suffering of the study's human and animal participants were minimized at all costs. The randomized human clinical trial registration number for *Phases 1/2* was *NCT00000381/ 2022*.

2.2. Type of the Study

Screening experimental study.

2.3. Place and Date of the Study

The study was conducted at Cairo University's pharmacy faculty in Egypt between *Julie 2022* and *November 2023*.

2.4. Source of Animal Models

The Department of Pharmacology and Toxicology at Cairo University's College of Pharmacy provided animal models, which were deemed acceptable.

2.5. Inclusion Criteria for Animal Models

Animal models of adult male, obese rabbits weighing approximately *2 kg* are available for Inoculation against several bacterial diseases. Before the trial, the rabbits were allowed to acclimatize for one week. At *50% ± 5%* humidity, *a 12-hour* light-dark cycle, and a regulated temperature of *25± 2°C*. Fresh grass was given to the bunnies to eat.

2.6. Exclusion Criteria for Animal Models

Young and female rabbits; Non-obese rabbits weighing less than *2 kg*.

2.7. Collection of 100 Soil Samples

The samples were randomly selected grassland soils that were taken from various soil settings in Egypt at a depth of 30 cm. Before being processed, samples were kept at 4 °C in sterile containers. Each soil sample was weighed out at one gram, and each *250 ml Erlenmeyer flask* had *99 ml* of sterile *distilled water*. The flasks were shaken at *400 rpm* for five minutes using a gyrator shaker. Following dilutions from 10^{-1} to 10^{-6} in sterile distilled water, the soil suspensions were plated on selective *Casein yeast peptone agar medium* (bought from *Sigma-Aldrich, USA*).

50 cc of *nutrient broth* liquid at *PH 7* was added to *250 ml Erlenmeyer flasks* to create the inoculum for the bacterial isolate under investigation. The medium was autoclaved and then infected with a loopful of culture from a nutritional agar slant that had been left overnight. The inoculum was the inoculated flasks, which were shaken for a whole day at *150 rpm*.

3. Instruments

3.1. Material

The suppliers of all chemical and biological materials were the Egyptian companies Alnasr Chemical Company and Algomhuria Pharmaceutical Company. Analytical-grade chemical reagents were utilized in all cases.

 doi:10.20944/preprints202405.0769.v1

Table 1. List of instruments.

Instrument	Model and manufacturer
Autoclaves	*Tomy, japan*
Aerobic incubator	*Sanyo, Japan*
Digital balance	*Mettler Toledo, Switzerland*
Oven	*Binder, Germany*
Deep freezer -70 ℃	*Artiko*
Refrigerator 5	*whirlpool*
PH meter electrode	*Mettler-toledo, UK*
Deep freezer -20 ℃	*whirlpool*
Gyrator shaker	*Corning gyrator shaker, Japan*
190-1100nm Ultraviolet-visible spectrophotometer	*UV1600PC, China*
Light(optical) microscope	*Amscope 120X-1200X, China*

3.2. Isolation of Corallococcus Coralloides DSM 2259 Producing Corallopyronin Antibiotics

The selective isolation of species of *Corallococcus coralloides DSM 2259* from different soil samples was directly achieved using dilution plating. The technique comprised the suppression of competing bacteria exploiting antibiotics such as *10 mcg/ ml Vancomycin* and/ or *10 mcg/ ml Chloramphenicol* combined with wet heat treatment of soils and air drying. Fungi were eliminated by supplementing the plating medium with *2 mcg/ ml Terbinafine HCl*. Swarming of *Corallococcus coralloides DSM 2259* colonies was controlled with *Casein Yeast Peptone* (*CYP*) plates incubated at *30℃* and *PH 7.2* for *5 days*. The constitution of *the CYP* plate included *0.4 % Peptone* from *Casein*, tryptically digested, *0.3 % CaCl2.2H2O*, *0.1 % MgSO4.7H2O*, *PH 7.2*. The potent bacterial isolate producing Myxopyronin was performed utilizing a *16 S rRNA* sequencing technique. The predominant bacterial isolate with high antibacterial activity was identified using *16S rRNA* sequencing and other biochemical tests. Nucleic acid was extracted from a swab by bead-beating in a buffered solution containing Phenol, Chloroform, and Isoamyl alcohol. The variable region of *the 16S rRNA* gene was then amplified from the resulting nucleic acid using *PCR*. The genomic *DNA* was extracted from *120 hours* of cultured cells using a *DNA purification kit*[*PurreLink™ Genomic DNA Mini Kit with Catalog number: K182002* was purchased from Invitrogen, USA] according to the protocol provided by the manufacturer of *the DNA* purification kit. *The 16S rRNA gene* was amplified by *PCR*[*PCR* SuperMix kit was purchased from Invitrogen, *USA*] using forward[*5-AGAGTTTGATCCTGGCTCAG-3-*] and reverse[*5-GGTTACCTTGTTACGACTT-3-*] *primers*. *PCR* amplicons from up to hundreds of samples were then combined and sequenced on a single run. The resulting sequences were matched to a reference database to determine relative bacterial abundances. Polymerase Chain Reaction (*PCR*) was a powerful method for amplifying particular segments of *DNA*. *PCR* used the enzyme *Platinum™ Taq DNA polymerase* with catalog number *10966018*[purchased from Invitrogen, *USA*] that directed the synthesis of *DNA* from deoxynucleotide substrates on a single-stranded *DNA template*. *DNA polymerase* added nucleotides to the 3` end of a custom-designed oligonucleotide when it was annealed to a longer template *DNA*. Thus, if a synthetic oligonucleotide was annealed to a single-stranded template that contained a region complementary to the oligonucleotide, *DNA polymerase* could use the oligonucleotide as a primer and elongate its 3` end to generate an extended region of double-stranded *DNA*. **Denaturation was the initial *PCR* cycle stage** The *DNA* template was heated to *94° C*. This broke down the weak hydrogen bonds that held *DNA* strands together in a helix, allowing the strands to separate creating single-stranded *DNA*. **Annealing was the second *PCR* cycle.** The mixture was cooled to anywhere from *50-70° C*. This allowed the primers to bind (anneal) to their complementary sequence in the template *DNA*. **The extension was the final step of *the PCR* cycle.** The reaction was; then heated up to *72° C*, the optimal temperature for *DNA polymerase* to act.

 doi:10.20944/preprints202405.0769.v1

*DNA polymeras*e extended the primers, adding nucleotides onto the primer in a sequential manner, using the target *DNA* as a template. *With one cycle, a single segment of double-stranded DNA template was amplified into two separate pieces of double-stranded DNA. These two pieces were then available for amplification in the next cycle. As the cycles were repeated, more and more copies were generated and the number of copies of the template was increased exponentially.* The amplified *PCR* product was sequenced using a genetic analyzer *3130XL*[purchased from Applied Biosystems, *USA*]. *DNA* sequence homology search analysis of the predominant bacterial isolate was achieved using the Blastn algorithm at *the NCBI* website. Fruiting bodies were examined using a *Stereomicroscope* (*dissecting microscope*) *MSC-ST45T* (purchased from Infetik, China). Wet mounts from crushed fruiting bodies were prepared. The refractivity, shape, and size of Myxospores were determined by employing phase contrast microscopy. On the other hand, the plates were exposed to *360 nm* wavelength ultraviolet light to assess the fruiting bodies fluoresced [16].

3.3. Identification of Myxopyronin B-Producing Bacterial Isolates

3.3.1. Gram Stain

It classified bacteria into two categories based on the makeup of their cell walls. The bacterial cells became purple after being treated with a solution of crystal violet and subsequently iodine on a microscope slide. When colored cells were treated with a solvent such as alcohol or acetone, gram-positive organisms kept the stain whereas gram-negative organisms lost the stain and turned colorless. With the addition of the counter-stain safranin, the clear, gram-negative bacteria became pink [17].

3.3.2. Spore Shape

This was discovered using the spore staining method. To get rid of any fingerprints, the slide was wiped with alcohol and a Kim wipe. On the bottom of the slide, a Sharpie was used to create two circles. Each circle was filled with two tiny droplets of water using an inoculation loop. A very small amount of germs was taken out of the culture tube using an aseptic method. The water droplet on the slide had microorganisms on it. The slide was thoroughly dried by air. Bypassing the slide through the flame three to four times with the smear side up, the slide was heat-fixed. It took a while for the slide to completely cool. A piece of paper towel placed inside the slide's border was used to hide the streaks. A beaker of heating water was situated over the slide. The slide was allowed to steam for three to five minutes; while the paper towel was covered with a malachite green liquid. Removed and thrown away was the discolored paper towel. To get rid of any stray paper towel bits, the slide was gently cleaned with water. The counter-stain was safranin for 1 minute. Before putting the slide on the microscope's stage and seeing it via the oil immersion lens, the slide's bottom was dried [18].

3.3.3. Spore Site

During the Gram stain test, the spore location was established [19].

3.3.4. Cell Shape

During the Gram stain test, the cell shape was assessed [20].

3.3.5. Blood Hemolysis

On blood agar media, the test antibiotic capacity to haemolyze the blood was tested [21].

3.3.6. Motility Test

It discriminated between motile bacteria and non-motile bacteria.

A sterile needle was used to penetrate the medium to within 1 cm of the tube's bottom to select a well-isolated colony and test for motility. The needle was certainly retained in the same position as

 doi:10.20944/preprints202405.0769.v1

it was inserted and removed from the medium. It took *18* hours of incubation at *35°C*, or until noticeable growth appeared [22].

3.3.7. Nitrate Reduction Test

0.5 ml of nitrate broth was added to a clean test tube, autoclaved for 15 minutes at *15 lbs pressure* and *121°C*, and let to cool to room temperature. The tube was inoculated with a heavy inoculum of fresh bacterial culture and was incubated at *35°C* for *2 hours*. *2 drops* of reagent A and *2 drops* of reagent B were added and mixed well. The development of a red color within *2 minutes* was observed. If no red color was developed, a small amount of *zinc dust* was added and observed for the development of the red color within *5 minutes* [23].

3.3.8. Methyl Red Test

In the Methyl Red test, an infected tube of *MR* broth was used before adding the methyl red *PH* indicator. The buffers in the medium were overcome by the acids when an organism used the mixed acid fermentation pathway and produced stable acidic end products, resulting in an acidic environment [24].

3.3.9. Catalase Test

A little inoculum of a specific bacterial strain was introduced to a *3%* hydrogen peroxide solution to see if it might produce catalase. It was observed for the rapid emergence of oxygen bubbles [25].

3.3.10. Oxidase Test

The 1% Kovács oxidase reagent was applied to a tiny piece of filter paper, which was then allowed to air dry. A well-isolated colony was taken from a fresh (*18 to 24-hour culture*) bacterial plate using a sterile loop, and it was then rubbed onto prepared filter paper. Color alterations were noticed [26].

3.3.11. Citrate Utilization

Five milliliters of a Simmon Koser's citrate medium were taken after it had been autoclaved at *15* pounds for *15 minutes*. To create a clear slant and butt, the test tube containing melted citrate medium was slanted. Using sterilized wire and labeled tubes, the specified samples of microbe were injected on the media's incline. For *24 hours*, the tubes were incubated at *37°C*. The medium's color shift was watched for [27].

3.3.12. Starch Hydrolysis

For *48 hours* at *37°C*, the bacterium plates were injected. After incubation, a dropper was used to saturate the surface of the plates with an iodine solution for *30 seconds*. Iodine that was in excess was afterward poured out. The area surrounding the bacterial growth line was looked at [28].

3.3.13. Tween 80 Hydrolysis

1% Tween 80 was used to create agar media. The supplied microorganism was added to the *Tween 80 agar plates* by utilizing an inoculating loop to create a single center streak in the plate. The plates were incubated for *24* hours at *37 °C*. *HgCl2* solution was poured over the plates. After a short while, the plates were examined. Positive test result; distinct halo-zone surrounding the injected region showed *Tween 80* hydrolysis [29].

3.3.14. Growth at 10-45℃

On nutrient agar media, growth was observed to be possible at *10-45°C* [30].

 doi:10.20944/preprints202405.0769.v1

3.3.15. Indole Test

The test tube containing the microorganism for inoculation received *5 drops* of the *Kovács reagent* directly. Within seconds after introducing the reagent to the media, the reagent layer formed a pink-to-red color (cherry-red ring), which was a sign of a positive indol test [31].

3.3.16. Tolerance Salinity Test

Its capacity to develop on nutrient agar while being responsive to *5%* and *7 % NaCl* was examined [32].

3.3.17. Voges-Proskauer(VP) Test

For the test, Voges-Proskauer broth, a glucose-phosphate broth loaded with microorganisms, was added to alpha-naphthol and potassium hydroxide. A successful outcome was indicated by a cherry red tint, whereas an unfortunate outcome was indicated by a yellow-brown color [33].

3.3.18. Casein Hydrolysis Test

For testing the casein hydrolyzing activity of the test antibiotic, a single line streak of the given culture was made in the center of the skim milk agar plate under aseptic conditions, and the plate was incubated at *37°C* in an incubator for *24-48 h* [34].

3.4. Saccharide Fermentation Tests

3.4.1. Glucose Fermentation Test

The fermentation reactions of glucose were investigated using glucose purple broth. Peptone and the *PH* indicator bromocresol purple made up the purple broth. A *1%* concentration of glucose was added. Isolated colonies from a *24-hour* pure culture of microorganisms were added to the glucose purple broth as an inoculant. Parallel to the inoculation of the glucose-based medium, a control tube of purple broth base was used. The inoculated medium was incubated aerobically for *3 days* at a temperature of *35–37* ℃. The medium began to become yellow, which was a sign of a successful outcome. A poor carbohydrate fermentation response was indicated by the lack of yellow color development [35].

3.4.2. Fructose Fermentation Test

A pure culture's inoculum was aseptically transferred to a sterile tube of phenol red fructose broth. The infected tube was incubated for *18–24 hours* at *35–37 °C*. A color shift from red to yellow, signifying an acidic PH alteration, was a sign of a favorable response [36].

3.4.3. Maltose Fermentation Test

A pure culture inoculum was aseptically transferred to a sterile tube containing phenol red maltose broth. The infected tube was incubated for *18–24 hours* at *35–37 °C*. A color shift from red to yellow, signifying an acidic PH alteration, was a sign of a favorable response [37].

3.4.4. Sucrose Fermentation Test

A pure culture's inoculum was aseptically transferred to a sterile tube containing phenol red sucrose broth. For *24 hours*, the infected tube was incubated at *35–37* ℃. A color shift from red to yellow, signifying an acidic *PH* alteration, was a sign of a favorable response [38].

3.4.5. Purification of Corallopyronin B Antibiotic

This was achieved through the reversed phase chromatography technique.

The aeration rate was *0.142 V/ V. min.* The stirring rate was *500 rpm*. *PO2* was at about *90 %* of saturation; but decreased to about *20 %* after *18 hours*). The fermentation was stopped after *40 hours*

 doi:10.20944/preprints202405.0769.v1

via centrifugation at *500 rpm* in a gyrator shaker. The supernatants were collected; and then tested for antimicrobial sensitivity using broth dilution technique to detect MICs and agar paper diffusion discs technique. The test antibiotic was extracted from the *2 liters* of culture broth with *2/ 10 volume* ethyl acetate. The ethyl acetate was then removed under the reduced pressure at *40 ℃*. Afterward, the residue was dissolved in 398 ml of methanol-water (*90: 10*) and chromatographed on reversed-phase *HPLC*. Methanol was the mobile phase. The eluent was *70* part *methanol*: *16* part *water*: *and 4* part *acetic acid* with a flow rate of *300 ml/ min*. Detection of the antibiotic components was achieved by exploiting the refractive index. The main peak with a retention time of *5 minutes* contained the biological antibiotic activity which was determined via agar diffusion assay using paper discs and *Staphylococcus aureus* as an indicator organism. On the other hand, the main peak was subjected to neutralization via *NaHCO3*. *Corallopyronin A* was extracted using *10 % V/ V Methylene chloride*. After the evaporation of the solvent, about *87 %* of the antibiotic substance purified was *Corallopyronin B*. It was noticed that the retention time of *Corallopyronin B* was *9 minutes*. The molecular formula of the purified *Corallopyronin B* was detected through a mass spectrometer (*Quadrupole mass spectrometer, Advion, USA*) [39]. It was detected also, that *13%* of *Corallopyronin mixture extract* were *7% Corallopyronin A* and 6% *Corallopyronin C*.

3.5. The Procedure of Broth Dilution Assay for Determination of MICs of Corallopyronin B

A specific broth was added to several microtiter plates during the testing process based on the requirements of the target bacterium. The test microorganisms and antibiotics were then introduced to the plate in varying amounts. After that, the plate was put into a non-*CO2* incubator and left there for *sixteen* to *twenty hours* at *37 degrees Celsius*. The plate was taken out and examined for bacterial growth after the specified amount of time had passed. Bacterial growth was detected in the cloudiness of the broth. The lowest concentration of antibiotics that prevented bacterial growth, or Minimum Inhibitory Concentration (*MIC*), was used to describe the outcomes of t*he broth microdilution* method [40].

3.6. Agar Diffusion Assay with Paper Discs Procedure for the Determination of Corallopyronin B Antimicrobial Activity

The agar diffusion technique (*ADM*) was used to classify the disc diffusion method (*DDM*) because the test microorganism-seeded agar media allowed the test antibiotic extract to disperse from its reservoir. A filter paper disc put on an agar surface served as the reservoir most of the time. After the filter paper disc was incubated, an inhibitory zone formed around the tested extract chemicals that were microbiologically active. The test extract's antibacterial potency was accurately reflected by the inhibition zone's diameter [41]. Both broth and selection or enrichment growing media were used to isolate the test microorganisms (Table 2).

Table 2. It demonstrates different isolation media for different pathogenic m.os. utilized in the *Broth microdilution* test and agar diffusion assay using paper discs:.

Pathogenic m.o	**No of strains**	**Isolation media**
Bacillus subtilis	*5*	*Mannitol egg yolk polymixin agar (MEYP)*
Bacillus cereus	*7*	*Polymixin egg yolk mannitol bromothymol blue agar (PEMBA)*
Staphylococcus aureus	*6*	*Salt mannitol agar (SMA)*
Pneumococci	*13*	*Todd Hewitt broth with yeast extract*

 doi:10.20944/preprints202405.0769.v1

E. coli	*17*	*Sorbitol- Macconkey agar*
Pseudomonas aeruginosa	*10*	*Pseudomonas isolation agar (PSA)*
Candida albicans	*1*	*Potato dextrose agar (PDA)*
Saccharomyces cerevisiae	*5*	*Sabourad dextrose agar (SDA)*
Salmonella typhimurium	*4*	*Bismuth sulfite agar (BSA)*
Haemophilus influenza	*3*	*Enriched chocolate agar*
Gonococci	*4*	*Thayer martin medium*
meningococci	*6*	*Mueller Hinton agar*
Serratia Marcescens	*4*	*Caprylate thallous agar medium*
Mucor hiemalis	*1*	*Potato dextrose broth*
Shigella dysenteriae	*8*	*Hekteon enteric agar*
Micrococcus luteus	*1*	*Tryptic soy agar*
Proteus mirabilis	*1*	*Blood agar*
Chlamydiae pneumonae	*1*	*Chlamydiae pneumonae Monkey cell culture*
Rickettsiae typhi	*1*	*Chicken embryos culture*

3.7. Estimation of Corallopyronin B Effect on Bacterial RNA Synthesis

The concentration of *RNA* isolated with *RNeasy Kits* (purchased from *QIAGEN, USA*) was determined by measuring the absorbance at *260 nm* in a spectrophotometer. An absorbance of 1 unit at *260 nm* corresponds to *40 µg* of *RNA* per ml (*A260 = 1 = 40 µg/ ml*) [42].

3.8. Estimation of Corallopyronin B Effect on Bacterial Protein Synthesis

Absorbance was measured at *205 nm* to calculate the protein concentration by comparison with a standard curve. A (*205*) method could be used to quantify total protein in crude lysates and purified or partially purified protein. The *UV* spectrophotometer was set to read at *205 nm* allowing *15 min* for the instrument to equilibrate. The absorbance reading was set to zero with a solution of the buffer and all components except the protein present. The protein solution was placed in the 1 ml cuvette and the absorbance was determined. The dilution and readings of samples were performed in duplicate. The matched cuvettes for samples and controls were utilized during the test procedure. The extinction coefficient of the protein was known, and the following equation was employed. $Absorbance = Extinction\ \ coefficient \times concentration\ \ of\ \ protein \times path\ \ length\ \ (1\ \ cm)$ to determine the concentration of the protein [43].

3.9. Estimation of Pharmacodynamic and Pharmacokinetic Effects of Corallopyronin B during Experimental Animal Testing in Preclinical Clinical Trials

In the present study, the pharmacokinetics and the pharmacodynamics of *Corallopyronin B* were evaluated after dosing in male rabbit animal models weighing about *2 kg*. Furthermore, compound concentrations were determined in target compartments, such as lung, kidney, and thigh tissue, using *LC-MS/ MS*. Based on the pharmacokinetic results, the pharmacodynamic profile of *Corallopyronin B* was assessed victimizing the standard neutropenic thigh and lung infection models [44].

 doi:10.20944/preprints202405.0769.v1

3.10. Estimation of Pharmacodynamic and Pharmacokinetic Effects of Corallopyronin B in Randomized Human Clinical Trials Phases 1/2

This study was conducted on *150* human volunteer subjects to show the bioavailability, pharmacokinetics, and pharmacodynamics of the test antibiotic. The study was designed as a randomized, single-dose, 2-treatment, 2-period crossover trial with a washout period of *1 week*. Blood samples were collected at *0* (*baseline*), *10*, *20*, and *40 minutes* and at *1*, *1.5*, *2*, *3*, *4*, *6*, *9*, *12*, and *24 hours* postdose. Plasma concentrations of the 4 drugs were measured by using a rapid chromatography-tandem mass spectrometry method. Pharmacokinetic parameters were calculated by using noncompartmental methods. Bioequivalence was determined if the *90 % CIs* of the log-transformed test/ reference ratios *AUC* (*0-26*), *AUC* (*0-∞*), and *Cmax* were within the predetermined range of *80%* to *125%*. Tolerability was assessed by using clinical parameters and subject reports Pharmacodynamic effects were evaluated through the determination of *MICs* via agar diffusion assay and broth dilution technique During *randomized human clinical trials phases 1/2* all utilized infectious bacterial cell counts were estimated spectrophotometrically [45].

3.11. Estimation of Phototoxicity, Mutagenicity, and Carcinogenicity of the Test Antibiotic

The phototoxicity of *Corallopyronin B* was determined via the *3T3 neutral red uptake phototoxicity* technique [46]. On the other hand, *mutagenicity* and carcinogenicity of the test antibiotic were assessed using *the Ames test* [47].

3.12. The Determination of Toxicokinetic and Toxicodynamic Effects

Up and down method for acute toxicity detection of *Corallopyronin B* was utilized for this purpose [48].

3.13. The Determination of the Maximum Bactericidal Activity of Corallopyronin B

A pure culture of a specified microorganism was grown overnight, then diluted in growth-supporting broth (typically *Mueller Hinton Broth*) to a concentration between *1 x 10^5* and *1 x 10^6 cfu/ ml*. A stock dilution of the antimicrobial test substance was made at approximately *100* times the expected *MIC*. Further *1:1* dilutions were made in test tubes. All dilutions of the test antibiotic were inoculated with equal volumes of the specified microorganism. A positive and negative control tube was included for every test microorganism to demonstrate adequate microbial growth over the course of the incubation period and media sterility, respectively. An aliquot of the positive control was plated and used to establish a baseline concentration of the microorganism used. The tubes were then incubated at the appropriate temperature and duration. Turbidity indicated growth of the microorganism and the *MIC* was the lowest concentration where no growth was visually observed. To determine the *MBC*, the dilution representing the *MIC* and at least two of the more concentrated test product dilutions were plated and enumerated to determine viable *CFU/ ml*. The *MBC* was the lowest concentration that demonstrated a pre-determined reduction (such as 99.9%) in *CFU/ ml* when compared to the *MIC* dilution [49].

3.14. Determination of Plasma Protein Binding Capacity of Corallopyronin B

Employing an ultrafiltration technique, the protein binding (*PB*) extent and changeability of the test antibiotic medicates were settled when given simultaneously to *30 patients* inoculated with infectious *pneumococci* inside hospitals in Egypt. Clinical samples used were routinely received by the microbiological laboratory inside the faculty of Pharmacy, Cairo University, Egypt. Plasma proteins were likewise plumbed. A protein-free medium was used to determine the nonspecific binding. Plasma samples from *30* patients were enclosed, of which plasma proteins were deliberated for *24 patients*.

 doi:10.20944/preprints202405.0769.v1

3.15. Determination of Liver, Kidney, and Heart Function Tests after the Addition of Corallopyronin B

These functional tests were performed to assess the vitality of *the liver*, *kidney*, and *heart* during the randomized human clinical trials phases *1/2*. On the other hand, Urine, and stool analyses were achieved in addition to the estimation of *complete blood counts* for all experimental subjects who received graded doses of *Corallopyronin B*.

3.16. Formulation of Corallopyronin B (COR B)

A liquid solution (COR B > 30 mg ml^{-1}) comprising polyethyleneglycol-15-hydroxy stearate (35%), propylene glycol (15%), and phosphate-buffered saline pH 7.3 (75%), as excipients, was prepared for IV and SC administration. PEG 400 (50%) and phosphate buffered saline pH 7.3 (60%) were added to a liquid formulation that included COR B for human effectuality attempts administered by oral and SC methods. For toxicity tests, a liquid COR B formulation based on PEG 200 that permitted an oral dosage of 1500 mg kg^{-1} (150 mg ml^{-1}) was created. Each formulation exhibited adequate COR B in-use stability.

4. Statistical Analysis

All cultures were conducted in triplets. Their presentation was by means and standard deviation. One-way analysis of variance ($p\ value \leq 0.05$) was used as a means for performing statistical analysis and also, statistical analysis was based on excel-spreadsheet-software. The *F statistical analysis test* was utilized during the present study.

5. Results

From the culture supernatant of the soil bacterial isolate *Corallococcus coralloides DSM 2259*, which was cultivated on a Casein yeast peptone (*CYP*) plate, *Corallopyronin B* was generated. The test antibiotic prevented the growth of various *Gram +ve* bacteria (*MICs* ranging from *1 to 10 mcg/ml*) and reduced the development of many *Gram -ve* bacteria (including *Escherichia coli*) at *MICs* more than *100* mcg/ml. Conversely, eukaryotic cells—such as those found in fungi and humans—were unaffected. By preventing bacterial *DNA-dependent RNA polymerase*, the test antibiotic was demonstrated to have a bactericidal effect (*RNLP*). When *600 mg* of the dose per *70 kg* of body weight was given *SC* in *phases 1/2 of randomized human clinical trials*, the *Cmax* was *8.6 mcg/ml* at *Tmax* of *one hour*; *T1/2* reached *136 mins* as a result of *first-order kinetics of elimination*. About *six to seven hours* after *SC* was given, it ceased working. Less than *6%* of experimental candidates experienced unusual toxicity in *phases 1/2* of the preclinical and randomized human clinical trials, manifested as decreased bile flow. A detectable *83%* protein binding with plasma albumin was found. After the test antibiotics were refined and purified using the *reverse phase HPLC technology*, Corallopyronin B was the predominant component (*Table 4*). *The 3T3 neutral red uptake phototoxicity test* was used to determine the phototoxicity, and it revealed no phototoxicity. However, the Ames test was used to determine the mutagenicity and carcinogenicity of the test antibiotic, and the results showed that there was no genotoxicity or carcinogenicity. The main isolates of *Gram-negative* bacteria that produce the antibiotic *Corallopyronin B* are shown using a stereomicroscope in *Figure 11*.

Tables 9 and 10, respectively, show that there was a considerable decrease in protein synthesis and *mRNA* synthesis as the dosage of Myxopyronin *B* was increased. Docking experiments with *the MCULE* and *SWISS DOCK software* showed that the test antibiotic's mechanism of action was most likely caused by inhibiting *RNA polymerase* by binding to its switch region. The test antibiotic's high *ΔG* was found to be roughly *15* J/mol using the SWISS-*MODEL software*. However, utilizing *SWISS-MODEL software*, it was discovered that the test antibiotic's low *Kd* near the switch area was roughly *-720 nM*. *Table 11* provides a summary of the biochemical profile and morphology of the strong bacterial isolates used in this investigation to produce the test antibiotic.

Corallococcus coralloides DSM 2259 was the most common bacterial isolate that secreted the extracellular test antibiotic, according to its appearance and biochemical responses. The study involved *150* human volunteers in total, with a mean age of *28.9*[*8.1*] years (*SD*). *The 88%* confidence

 doi:10.20944/preprints202405.0769.v1

intervals (*CIs*) for the long transformed ratios of Cmax, *AUC (0-26), and AUC (0-∞)* for the test antibiotic were, in order, *93.3* to *94.6, 90.5 to 95.2, and 90.7 to 93.1*. *Corallopyronin B* was found to have a mean protein binding (*PB)* of about *83%*. It was shown that *Albumin* exhibited the predominant protein binding for both Rifampicin and *Corallopyronin B*. The therapeutic activity was discovered to be attributed to the unbound fraction. The structure of *Corallopyronin B*, which was isolated from bacterial isolates of *Corallococcus coralloides DSM 2259* collected from various soil conditions in Egypt, is depicted in *Figure 1*. Using a mass spectrometer, the molecular formula of the purified test antibiotic was found to be $C_{31}H_{43}NO_7$. The area under the curve (*AUC*) after *oral Corallopyronin B* dosing during *phases 1/2* of clinical trials is shown in *Figure 9*. The range of effective doses was *9.5–10 mg/kg* of body weight. The action started after over thirty minutes. It adhered to the kinetics of first-order elimination. The quantal dosage response curve for the assessment of *Corallopyronin B's toxicokinetics* is displayed in *Figure 10*. It was discovered that LD_{50}% was *150 mg/kg* and LD_{99}% was around *310 mg/kg*. *The AUC* of *Corallopyronin B* after *SC* injection in *phases 1/2* of randomized human clinical trials is displayed in *Figure 8*. The range of effective doses was *8–9 mg/kg* of body weight. The beginning of the action was noted after a close *15 minutes*. It adhered to the kinetics of first-order elimination. The docking of the *Corallopyronin B ligand* on Bacterial *RNA polymerase* is shown in *Figure 2*. High affinity and an inhibitory impact were demonstrated by *Corallopyronin B* towards the *RNA Polymerase* switch region. *Figure 7* uses the *UV* spectrophotometer absorbance at *205 nm* to illustrate how *Corallopyronin B* affects protein synthesis. A significant reduction in protein synthesis was seen upon administration of escalating dosages of the antibiotic *Corallopyronin B*. *The three-dimensional structure* of bacterial prokaryotic *RNA polymerase* is depicted in *Figure 3*. This structure includes the switch binding site, to which *Corallopyronin B Ligand* binds strongly, inhibiting the activity of bacterial *RNA polymerase* selectively, which in turn causes the inhibition of *mRNA* transcription and ultimately the death of the microbe. *Alpha* and *Beta* spiral sheets make up the *RNA polymerase* enzyme's secondary structure. It had a molecular mass of about *198 amino acids*. *Figure 6* speaks about estimating Corallopyronin B's impact on the productivity of microbial *mRNA*. An increase in the dosage of the antibiotic *Myxopyronin B* was found to cause a commensurate decrease in *mRNA* production. The effects of varying peptone concentrations as a nitrogen growth factor on *Corallopyronin B* production are depicted in *Figure 5*. The effect of different soluble starch concentrations on the synthesis of *Corallopyronin B* is depicted in *Figure 4*. The resolution of biological reactions is shown in *Table 11*. *Table 8* uses *the Broth microdilution technique* to show the minimum bactericidal concentrations (*MBCs*) of *Corallopyronin B* on various bacteria. The measurement of the amount of *mRNA* using a *UV* spectrophotometer at *260 nm* following the addition of *Corallopyronin B* is displayed in Table 9. The distribution of bacterial isolates that produce *Corallopyronin B* is displayed in *Table 3*. The degree of purity of the test antibiotics after they were purified using *the reversed-phase HPLC process* is shown in *Table 4*. *Table 5* shows how to use *BLASTn software* to detect *16S rRNA* in isolates that produce *Corallopyronin B*. *Table 7* shows *Corallopyronin B's* minimum inhibitory concentrations (*MICs*) on several bacteria using the broth microdilution method. *Corallopyronin B's* zones of inhibition and minimum inhibitory concentrations are estimated using the Agar diffusion assay with paper discs, as shown in *Table 6*.

 doi:10.20944/preprints202405.0769.v1

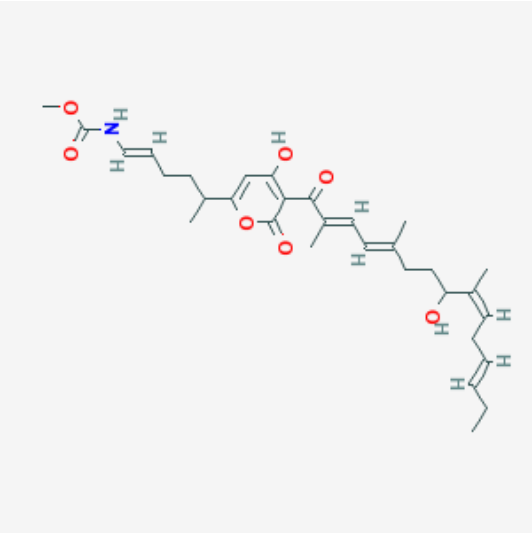

Figure 1. It demonstrates the structure of *Corallopyronin B* extracted from bacterial isolates *Corallococcus coralloides DSM 2259* collected from different soil environments in Egypt. The molecular formula of the purified test antibiotic was noticed to be $C_{31}H_{43}NO_7$ determined through a mass spectrometer.

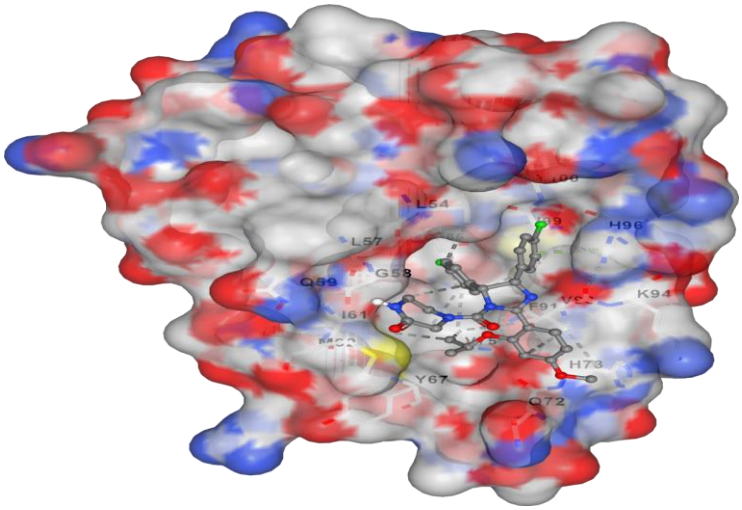

Figure 2. It represents *the docking* of *Corallopyronin B* ligand on Bacterial *RNA* polymerase. *Corallopyronin B* showed high affinity and inhibitory effect towards *the switch region* of *RNA Polymerase*. The molecular mass of *Corallopyronin B* was observed to be nearly *540 Da. ΔG* was found to be roughly *15* J/mol; nevertheless, it was discovered that the test antibiotic's *Kd* near the switch area was roughly *-720 nM*.

 doi:10.20944/preprints202405.0769.v1

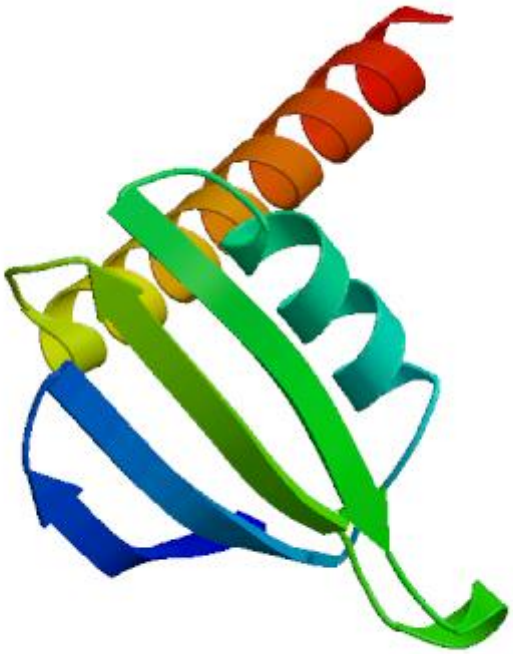

Figure 3. It demonstrates the 3*D* structure of bacterial prokaryotic *RNA polymerase* comprising the switch binding site to which *Corallopyronin B Ligand* is strongly bound inhibiting bacterial *RNA polymerase* activity selectively leading to the inhibition of *mRNA* transcription and subsequently the mortality of the microbe. The secondary structure of *the RNA polymerase* enzyme consisted of spiral *alpha* and *beta* sheets. Its molecular mass was approximately *198 amino acids*.

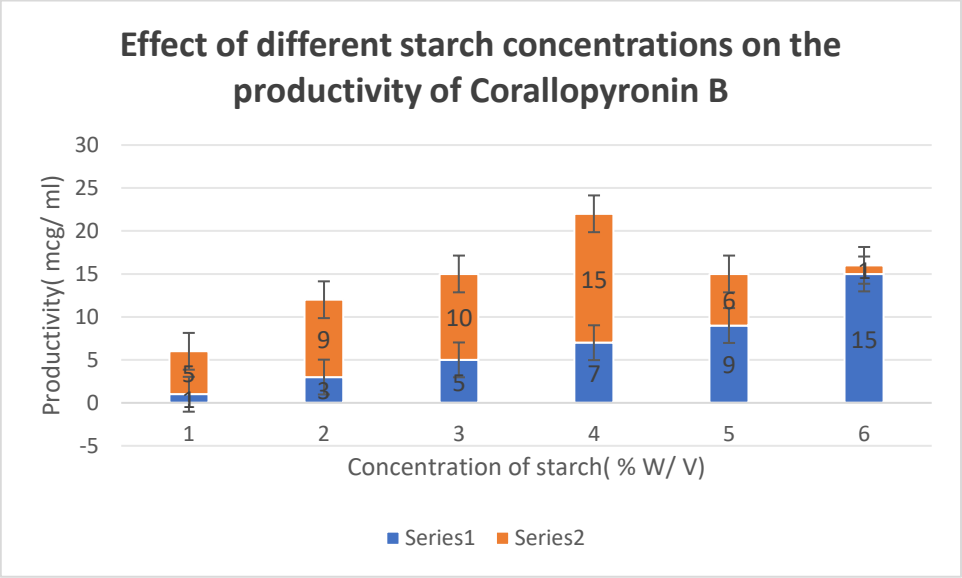

Figure 4. It shows the impact of various concentrations of *Soluble starch* on the production of *Corallopyronin B*.

Preprints.org (www.preprints.org) | NOT PEER-REVIEWED | Posted: 13 May 2024 doi:10.20944/preprints202405.0769.v1

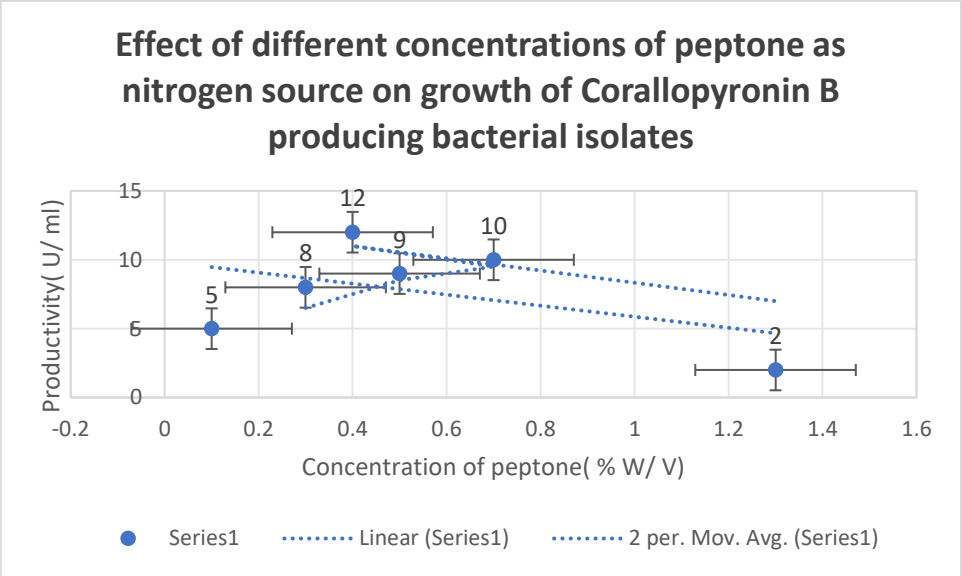

Figure 5. It shows the effects of different *Peptone* concentrations as a nitrogen growth factor on the productivity of *Corallopyronin B*.

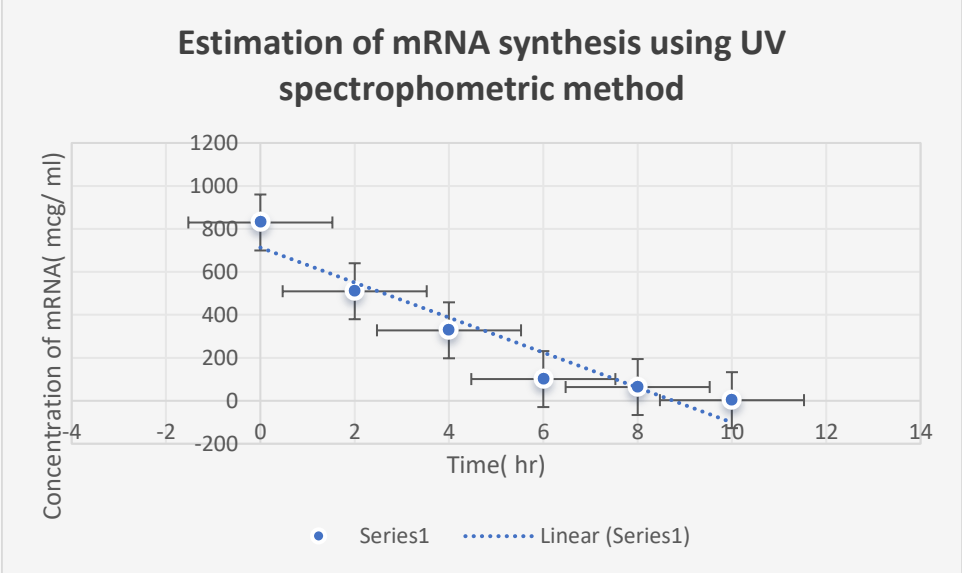

Figure 6. It refers to the estimation of the effect of *Corallopyronin B* on microbial *mRNA* productivity. *mRNA* synthesis was detected to be diminished proportionately upon employment of exploding doses of *Myxopyronin B* antibiotic.

 doi:10.20944/preprints202405.0769.v1

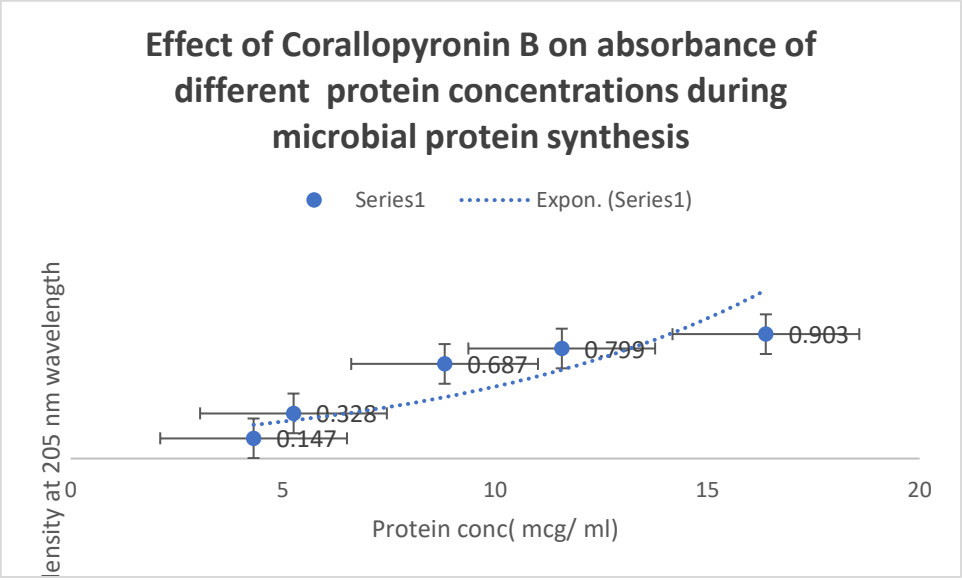

Figure 7. It demonstrates the influence of *Corallopyronin B* on protein synthesis using *UV* spectrophotometer absorption at *205 nm*. Protein synthesis was noticed to be decreased dramatically upon utilization of increasing doses of *Corallopyronin B* antibiotic.

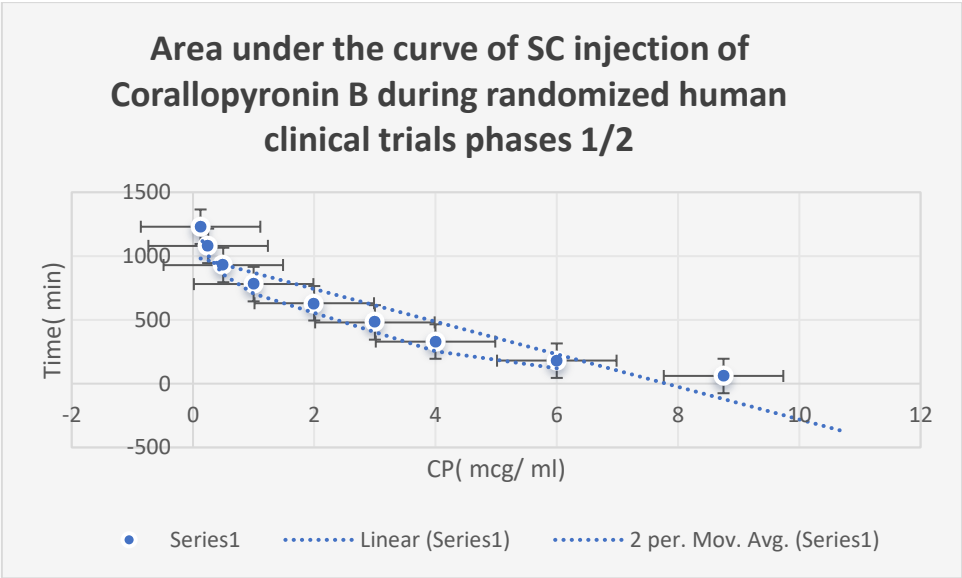

Figure 8. It shows *the AUC* of *Corallopyronin B* following *SC administration in randomized human clinical trials stages 1/2*. Efficacious dose ranged from *8-9 mg/ kg* of body weight. The onset of action was observed following closely *15 minutes*. It followed the *first order of elimination kinetics*. Bioavailability approximately reached *96%*.

Preprints.org (www.preprints.org) | NOT PEER-REVIEWED | Posted: 13 May 2024 doi:10.20944/preprints202405.0769.v1

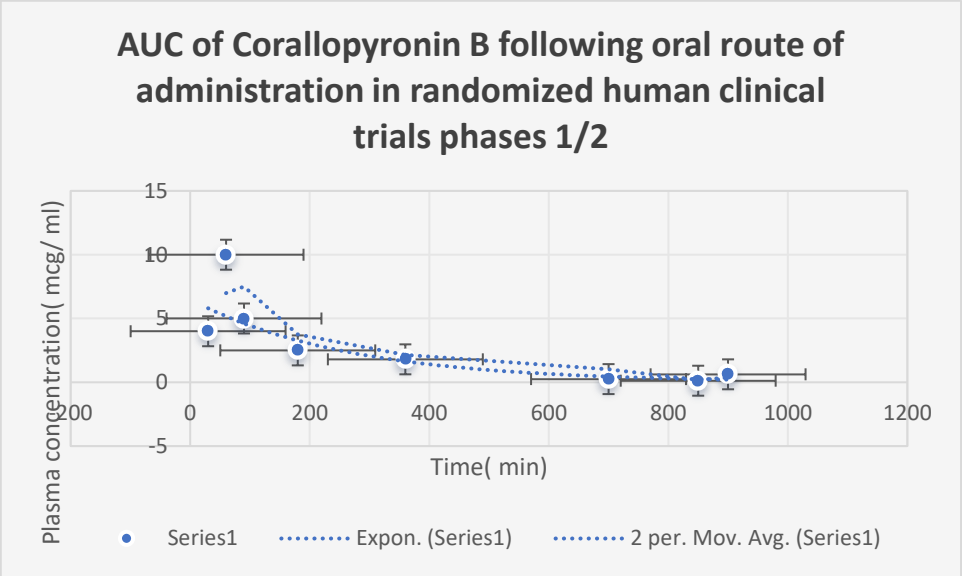

Figure 9. Area under the curve (*AUC*) following oral administration of *Corallopyronin B* during *clinical trials phases 1/2*. Efficacious dose ranged from *9.5-10 mg/ kg* of body weight. The onset of action was observed following nearly *30 minutes*. It followed the *first order of elimination kinetics*. Bioavailability reached approximately *95%*.

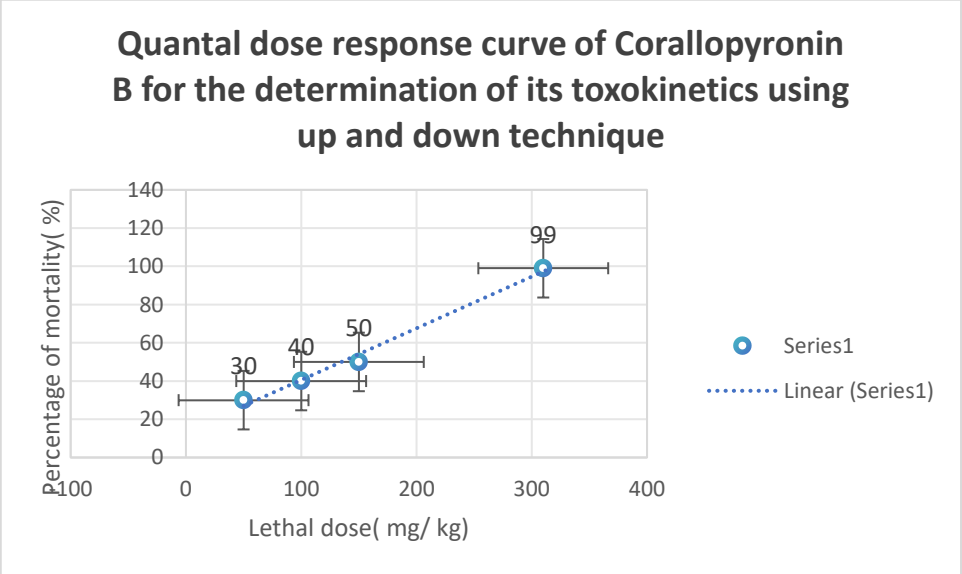

Figure 10. The quantal dose-response curve for the determination of toxicokinetics of *Corallopyronin B*. LD_{50} % was found to be 150 *mg/kg;* while *LD99* % was nearly *310 mg/ kg*.

Figure 11. It demonstrates the major *Gram-negative* bacterial isolates producing *Corallopyronin B* antibiotic using *a Stereomicroscope*.

 doi:10.20944/preprints202405.0769.v1

Table 3. It shows the distribution of *Corallopyronin B*-producing bacterial isolates.

No of +*ve* bacterial isolates producing *Corallopyronin A*	**No of -*ve* bacterial isolates producing *Corallopyronin A***
61	39

Table 4. It demonstrates the degree of purity of test antibiotics following the purification via *the reversed-phase HPLC technique*:.

Test antibiotic	**Degree of purity (%)**
Corallopyronin A	*7*
Corallopyronin B	*90*
Corallopyronin C	*3*

Table 5. It demonstrates *16 S rRNA* detection of *Corallopyronin B*-producing isolates using *BLASTn* software.

Description	Query Cover	E value	Per. ident	Acc. Len
Corallococcus coralloid's DSM 2259, complete genome	*100%*	*0*	*100*	*10080619*
Corallococcus sp. NCRR chromosome, complete genome	*100%*	*0*	*99.05*	*9787125*
Corallococcus coralloid's strain B035 chromosome, complete genome	*100%*	*0*	*98.57*	*9587888*
Corallococcus sp. EGB chromosome, complete genome	*100%*	*0*	*96.83*	*9431171*
Myxococcus fulvus 124B02, complete genome	*100%*	*0*	*92.08*	*11048835*
Myxococcus sp. MH1 DNA, complete genome	*100%*	*0*	*91.92*	*10778154*
Myxococcus sp. SDU36 chromosome, complete genome	*100%*	*0*	*91.63*	*9016985*
Myxococcus xanthus strain GH3.5.6c2 chromosome, complete genome	*100%*	*0*	*91.28*	*9321034*
Vulgatibacter incomptus strain DSM 27710, complete genome	*99%*	*2.00E-153*	*82.99*	*4350553*
Anaeromyxobacter sp. Fw109-5, complete genome	*99%*	*1.00E-125*	*80.43*	*5277990*
Uncultured bacterium clone F5K2Q4C04IF4QS 23S	*77%*	*3.00E-122*	*83.53*	*492*

 doi:10.20944/preprints202405.0769.v1

ribosomal RNA gene, partial sequence				
Uncultured bacterium clone F5K2Q4C04I5GUV 23S ribosomal RNA gene, partial sequence	*77%*	*6.00E-114*	*82.73*	*491*

Table 6. It shows the estimation of zones of inhibition and minimum inhibitory concentrations of *Corallopyronin B* via *Agar diffusion* assay using *paper discs*.

Test organism [1]	***MIC* (*μg/ ml*)**	**Diameter of inhibition zone (*mm*)**
Bacillus subtilis	*5*	*10*
Staphylococcus aureus	*6*	*16*
Streptococcus pneumonae	*10*	*7*
Escherichia coli	*119*	*13*
Pseudomonas aeruginosa	*129*	*0*
Candida albicans	*114*	*0*
Sacchromyces cerevisiae	*109*	*0*
Salmonella typhimurium	*137*	*15*
Bacillus cereus	*14*	*12*
Micrococcus luteus	*18*	*7*
Serratia Marcescens	*140*	*10*
Mucor hiemalis	*0*	*19*
Shigella dysentery	*109*	*14*
Proteus mirabilis	*123*	*8*
Rickettsiae prowazaki	*146*	*11*
Chlamydiae pneumonae	*125*	*19*
Legionella pneumophilla	*116*	*9*

[1] The initial density of each organism during the Agar diffusion assay for the determination of minimum inhibitory concentrations and zones of inhibition of growth was nearly 10^5/ ml.

Table 7. It demonstrates *MICs* of *Corallopyronin B* on different microorganisms using broth microdilution techniqu:.

Pathogenic m.o	***MIC* (*μg/ ml*)**
Bacillus subtilis	10
Bacillus cereus	7
Staphylococcus aureus	9
Pneumococci	6
E.coli	127
Pseudomonas aeruginosa	0
Candida albicans	0

 doi:10.20944/preprints202405.0769.v1

Sacchromyces cerevisiae	0
Salmonella typhimurium	109
Haemophilus influenza	0
Gonococci	105
meningococci	134
Serratia Marcescens	129
Mucor hiemalis	0
Shigella dysenteriae	111
Micrococcus luteus	0
Proteus mirabilis	0
Rickettsiae prowazaki	*139*
Chlamydiae pneumonae	*131*
Legionella pneumophilla	*146*

Table 8. It demonstrates Minimum *bactericidal* concentrations (*MBCs*) of *Corallopyronin B* on different microorganisms using *the Broth microdilution technique*.

Pathogenic m.o	***MBC* (*μg/ ml*)**
Bacillus subtilis	24
Bacillus cereus	23
Staphylococcus aureus	39
Pneumococci	44
E.coli	338
Pseudomonas aeruginosa	399
Candida albicans	0
Sacchromyces cerevisiae	0
Salmonella typhimurium	320
Haemophilus influenza	0
Gonococci	380
meningococci	377
Serratia Marcescens	307
Mucor hiemalis	0
Shigella dysenteriae	309
Micrococcus luteus	0
Proteus mirabilis	0
Rickettsiae prowazaki	*400*
Chlamydiae pneumonae	*416*
Legionella pneumophilla	*252*

Table 9. It shows the estimation of *mRNA* quantity via *UV* spectrophotometer at *260 nm* after the addition of *Corallopyronin B*.

 doi:10.20944/preprints202405.0769.v1

mRNA concentration (*ng/ ml*)	*Absorbance* (*optical density*) at *260 n*m
600	0.729
567	0.501
204	0.247
25	0.093

Table 10. It shows the effect of *Corallopyronin A* on microbial protein synthesis using a *UV* spectrophotometer at *205 nm*.

Bacterial protein concentration (mc*g/ ml*)	Time (hr)
91.3	2
45.96	4
28.38	7
3.37	10
0.26	3

Table 11. The resolution of biochemical reactions.

Test	Result
Gram stain	*-ve rods*
Cell shape	Elongated bacilli with tapered ends
Spore shape	Ellipsoidal
Spore site	Central
Motility	+ via gliding
Catalase	+
Oxidase	-
Blood haemolysis	-
Indol	-
Methyl red	-
Nitrate reduction test	+
Vogues Proskauer	-
Citrate utilization	-
Starch hydrolysis	+
Casein hydrolysis	+
Growth at 45 ℃	Bacterial isolates did not grow at 45 ℃; but were grown at 10-37 ℃
Tween 80	+
Tolerance salinity	
5% NaCl	-
7% NaCl	-
Saccharide fermentation	
Glucose	-

 doi:10.20944/preprints202405.0769.v1

Fructose	-
Maltose	-
Sucrose	-

6. Discuss

Globally, exploding morbidity and mortality due to antibiotic-resistant micro-organism infections were observed. Hence, amended hindrance and touchstone of infectious diseases, as well as appropriate use of approved antibacterial drugs were essential. The in vitro and in vivo antimicrobial activity of *Corallopyronin B*, a novel antibiotic was evaluated in the present study. It demonstrated excellent bactericidal activity against a broad spectrum of *G +ve bacteria* with *MICs* that did not exceed *20 mcg/ ml*. On the other hand, It showed broad bactericidal activities against *G -ve bacteria* with minimal inhibitory concentrations greater than *100 mcg/ ml*. Its mechanism of action was realized during the investigation of *RNA synthesis* to be via the inhibition of prokaryotic *DNA-dependant-RNA polymerase*; whereas no inhibitory impact was observed for Eukaryotic one. Docking studies through *SWISS DOCK* software confirmed this as well. The antibiotic activities *Corallopyronin A, B,* and *C* were isolated from the culture supernatant of *29* bacterial isolates of Myxobacterium *Corallococcus coralloides DSM 2259* detected molecularly using *16 S rRNA* technique (Table 3). The antibiotic activity did not inhibit the growth or kill eukaryotic cells such as human and fungal cells reflecting selectivity towards the inhibition of the growth of prokaryotic bacterial cells. This selectivity effect minimized the adverse effects noticed during the present study. Docking studies via *SWISS DOCK* software revealed that desmethylation of either Corallo*pyronin A, B, or C* enhanced its biological activity. Purification was performed through reversed-phase *HPLC*. Corallo*pyronin B* was the main refined antibiotic. Its purity degree reached approximately *90 %*; while the remaining purified antibiotics were detected to be *Corallopyronin A (7 %) and C (3 %)*. The antibacterial activity was assessed via the determination of *MICs* of the test antibiotics using the agar diffusion technique utilizing paper discs *5 mm* in diameter and the broth dilution assay. The initial density of each test microorganism was about 10^5*/ ml* of the culture suspension. The *MICs* of test antibiotics against *G +ve bacteria* ranged from *6* to *20 mcg/ ml;* Whereas *MICs* reached above *100 mcg/ ml* against some selected *G -ve bacteria.* On the other hand, no effect was detected against the growth of fungi and yeasts. (Irschik H et al., 1983) stated that *Myxovalargin A* was a novel peptide antibiotic isolated from the culture supernatant of the *myxobacterium Myxococcus fulvus strain Mx f65*. It was active against *Gram-positive bacteria* (*MIC 0.3* approximately *5 micrograms/ ml*), at higher concentrations also against *Gram-negative* ones (*MIC 6 approximately 100 micrograms/ ml)*, and not at all against yeasts and molds. Its mechanism of action involved the inhibition of bacterial protein synthesis [50]. According to (Glaus F et al., 2018) *Ripostatin*, a novel antibiotic, isolated from the culture supernatant of *Myxobacterium*, *Sorangium cellulosum strain So ce377*. On the other hand, it interfered with the bacterial *RNA* synthesis [51]. On the other hand, *Corallopyronin B* was found to be structurally related to *α-pyrone* antibiotics from *myxobacteria*. Its ability to inhibit *RNA polymerase* was through interaction with the switch region of *RNA polymerase*; while *Rifampicin* inhibited the same enzyme through different regions [52]. Myxopyronin showed no phototoxicity and mutagenicity in rabbit animal models during *the preclinical trials stage*, in the present study. Rare adverse effects including cholestatic jaundice were reported in less than *5 %* of the experimental subjects who received the test antibiotics during *randomized human clinical trials phases 1/2*. The biological half-life of *Corallopyronin B* reached approximately *2.25 hours*. *0.4 % peptone* and *7 % soluble starch* were detected to be the optimal nitrogen and carbon growth factors for bacterial isolates producing the test antibiotics, respectively (*Figures 4 and 5*). The high *ΔG* of the test antibiotic was observed to be approximately *15 J/ mole* as determined via *SWISS-MODEL* software reflecting high catalytic activity of the test antibiotic towards the switch region. On the other hand, low *Kd* of the test antibiotic towards the switch region was found to be approximately *-720 nM* using *SWISS MODEL* software indicating high affinity and binding capacity. Bioavailability studies were performed using *HPLC* during randomized human clinical trials phases *1/2* revealed that *Corallopyronin B* reached nearly *95% oral bioavailability*, 96% *IM bioavailability*, and

 doi:10.20944/preprints202405.0769.v1

100% IV bioavailability. Metabolic studies using *HPLC* revealed that the test antibiotic showed no in vivo induction of hepatic metabolizing C*ytochrome P450* enzymatic system; while *Rifampicin* induced *CYP3A4* hepatic metabolizing enzyme potently. Up and down procedure intended for the evaluation of the acute toxicity profile of the test antibiotic showed that LD_{50}% was about *150 mg/ kg* body weight; while LD_{99}% reached *310 mg/ kg*. On the other hand, the therapeutic margin of the test antibiotic ranged from 7 *mcg/ ml* to *100 mcg/ ml*. *Corallopyronin B*-producing bacterial isolates were gram-negative, spore-forming *obligate aerobes* and *chemoorganotrophic*. They were *elongated rods* with *tapered ends*. No *flagella* were present, but the cells moved via *gliding*. They fermented *Tween 80*, *starch*, and *casein*. On the other hand, they were positive for *catalase* while negative for *oxidase* tests. They reduced *nitrates*

And were able to grow at *10-37 ℃*. A total of *150* human subjects (mean *SD* age, *27.3*[*8.6*] years were enrolled and completed the study. *The 88%* confidence intervals (*CIs*) for the long transformed ratios of *Cmax*, *AUC (0-26), and AUC (0-∞)* for the test antibiotic were, in order, *93.3* to *94.6, 90.5 to 95.2, and 90.7 to 93.1, respectively*. The point estimates for *Cmax* in the present study were outside the limit for bio-equivalence for the *Rifampicin* standard drug. The mean *PB* was observed for *Corallopyronin B* which approximated 83% while that of *Rifampicin* reached *88%* [53]. It was noticed that plasma protein binding was proportionally increased with increasing the doses of the test antibiotic. The plasma protein binding participated in extending the *Corallopyronin B* duration of action. The major protein binding for *Corallopyronin B* and *Rifampicin* was noticed to be *Albumin*. The unbound fraction was detected to be responsible for the therapeutic activity.

7. Conclusions

Antibiotic resistance is a global challenge that the current study shows promise in solving. According to the findings of the current study, *Corallopyronin B*, which was isolated from the bacterial isolates *Corallococcus coralloides DSM 2259* that were collected from various soil environments in Egypt, exhibited significant antibiotic activity both in vitro and in vivo against a moderate range of pathogenic bacteria, particularly *G+ve* varieties. Future research is recommended to investigate pharmacological interactions of the synergism type between *Corallopyronin A* and different antibiotic classes.

8. Patents

Corallopyronin B produced from the bacterial isolates *Corallococcus coralloides DSM 2259* that were collected from different soil environments in Egypt, evidenced fundamental antibiotic activity both in vitro and in vivo versus a moderate scope of infective micro-organisms, peculiarly *G+ve* miscellanea.

Author contribution: This study was achieved completely by the single author, Prof. Mohammed Kassab.

Funding: This study was funded by the single author, Prof. Mohammed Kassab.

Institutional Review Board statement: The study was conducted in accordance with the Declaration of Helsinki and approved by Ethics committee; as well as all relevant institutional, national, and/ or worldwide standards on the use and care of humans and animals were given priority in the current study. The Ethical Committee for Human and Animal Handling at Cairo University (*ECAHCU*), housed at the Faculty of Pharmacy, Cairo University, Egypt, approved all study procedures involving humans and animals per the recommendations of the Weatherall Report (approval number *T716-2022*). The number and degree of suffering of the study's human and animal participants were minimized at all costs. The randomized human clinical trial registration number for *Phases 1/2* was *NCT00000381/ 2022*.

Informed Consent Statement: Written informed consent was obtained from all patients to publish this paper; as well as informed consent was obtained from all subjects involved in the study.

 doi:10.20944/preprints202405.0769.v1

Data Availability Statement: All data supporting the reported results are included within the manuscript.

Acknowledgement: Faculty of Pharmacy, Cairo University, Egypt are acknowledged due to their support to achieve the present study.

References

1. Dalhoff A. Selective toxicity of antibacterial agents-still a valid concept or do we miss chances and ignore risks? Infection. 2021 Feb;49(1):29-56. doi: 10.1007/s15010-020-01536-y. Epub 2020 Dec 23. PMID: 33367978; PMCID: PMC7851017.
2. Hutchings MI, Truman AW, Wilkinson B. Antibiotics: past, present and future. Curr Opin Microbiol. 2019 Oct;51:72-80. doi: 10.1016/j.mib.2019.10.008. Epub 2019 Nov 13. PMID: 31733401.
3. Wencewicz TA. Crossroads of Antibiotic Resistance and Biosynthesis. J Mol Biol. 2019 Aug 23;431(18):3370-3399. doi: 10.1016/j.jmb.2019.06.033. Epub 2019 Jul 6. PMID: 31288031; PMCID: PMC6724535.
4. Lepe JA, Martínez-Martínez L. Resistance mechanisms in Gram-negative bacteria. Med Intensiva (Engl Ed). 2022 Jul;46(7):392-402. doi: 10.1016/j.medine.2022.05.004. Epub 2022 May 31. PMID: 35660283.
5. Vila J, Marco F. Lectura interpretada del antibiograma de bacilos gramnegativos no fermentadores [Interpretive reading of the non-fermenting gram-negative bacilli antibiogram]. Enferm Infecc Microbiol Clin. 2010 Dec;28(10):726-36. Spanish. doi: 10.1016/j.eimc.2010.05.001. Epub 2010 Jun 26. PMID: 20579775.
6. Mushtaq S, Vickers A, Woodford N, Livermore DM. WCK 4234, a novel diazabicyclooctane potentiating carbapenems against Enterobacteriaceae, Pseudomonas, and Acinetobacter with class A, C, and D β-lactamases. J Antimicrob Chemother. 2017 Jun 1;72(6):1688-1695. doi: 10.1093/jac/dkx035. PMID: 28333319.
7. Irwin SV, Fisher P, Graham E, Malek A, Robidoux A. Sulfites inhibit the growth of four species of beneficial gut bacteria at concentrations regarded as safe for food. PLoS One. 2017 Oct 18;12(10):e0186629. doi: 10.1371/journal.pone.0186629. PMID: 29045472; PMCID: PMC5646858.
8. Jeong S, Lee Y, Yun CH, Park OJ, Han SH. Propionate, together with triple antibiotics, inhibits the growth of Enterococci. J Microbiol. 2019 Nov;57(11):1019-1024. doi: 10.1007/s12275-019-9434-7. Epub 2019 Oct 28. PMID: 31659687.
9. Kohanski MA, Dwyer DJ, Hayete B, Lawrence CA, Collins JJ. A common mechanism of cellular death induced by bactericidal antibiotics. Cell. 2007 Sep 7;130(5):797-810. doi: 10.1016/j.cell.2007.06.049. PMID: 17803904.
10. Brauer M, Herrmann J, Zühlke D, Müller R, Riedel K, Sievers S. Myxopyronin B inhibits the growth of a Fidaxomicin-resistant Clostridioides difficile isolate and interferes with toxin synthesis. Gut Pathog. 2022 Jan 6;14(1):4. doi: 10.1186/s13099-021-00475-9. PMID: 34991700; PMCID: PMC8739712.
11. Doundoulakis T, Xiang AX, Lira R, Agrios KA, Webber SE, Sisson W, Aust RM, Shah AM, Showalter RE, Appleman JR, Simonsen KB. Myxopyronin B analogs as inhibitors of RNA polymerase, synthesis, and biological evaluation. Bioorg Med Chem Lett. 2004 Nov 15;14(22):5667-72. doi: 10.1016/j.bmcl.2004.08.045. PMID: 15482944.
12. Lira R, Xiang AX, Doundoulakis T, Biller WT, Agrios KA, Simonsen KB, Webber SE, Sisson W, Aust RM, Shah AM, Showalter RE, Banh VN, Steffy KR, Appleman JR. Syntheses of novel myxopyronin B analogs as potential inhibitors of bacterial RNA polymerase. Bioorg Med Chem Lett. 2007 Dec 15;17(24):6797-800. doi: 10.1016/j.bmcl.2007.10.017. Epub 2007 Oct 17. PMID: 17980587.
13. Moy TI, Daniel A, Hardy C, Jackson A, Rehrauer O, Hwang YS, Zou D, Nguyen K, Silverman JA, Li Q, Murphy C. Evaluating the activity of the RNA polymerase inhibitor myxopyronin B against Staphylococcus aureus. FEMS Microbiol Lett. 2011 Jun;319(2):176-9. doi: 10.1111/j.1574-6968.2011.02282.x. Epub 2011 Apr 20. PMID: 21477256.
14. Srivastava A, Talaue M, Liu S, Degen D, Ebright RY, Sineva E, Chakraborty A, Druzhinin SY, Chatterjee S, Mukhopadhyay J, Ebright YW, Zozula A, Shen J, Sengupta S, Niedfeldt RR, Xin C, Kaneko T, Irschik H, Jansen R, Donadio S, Connell N, Ebright RH. New target for inhibition of bacterial RNA polymerase: 'switch region'. Curr Opin Microbiol. 2011 Oct;14(5):532-43. doi: 10.1016/j.mib.2011.07.030. Epub 2011 Aug 19. PMID: 21862392; PMCID: PMC3196380.
15. Mosaei H, Harbottle J. Mechanisms of antibiotics inhibiting bacterial RNA polymerase. Biochem Soc Trans. 2019 Feb 28;47(1):339-350. doi: 10.1042/BST20180499. Epub 2019 Jan 15. PMID: 30647141.
16. Sucipto H, Sahner JH, Prusov E, Wenzel SC, Hartmann RW, Koehnke J, Müller R. In vitro reconstitution of α-pyrone ring formation in myxopyronin biosynthesis. Chem Sci. 2015 Aug 1;6(8):5076-5085. doi: 10.1039/c5sc01013f. Epub 2015 May 18. PMID: 29308173; PMCID: PMC5724707.
17. O'Toole GA. Classic Spotlight: How the Gram Stain Works. J Bacteriol. 2016 Nov 4;198(23):3128. doi: 10.1128/JB.00726-16. PMID: 27815540; PMCID: PMC5105892.
18. Luhur J, Chan H, Kachappilly B, Mohamed A, Morlot C, Awad M, Lyras D, Taib N, Gribaldo S, Rudner DZ, Rodrigues CDA. A dynamic, ring-forming MucB / RseB-like protein influences spore shape in Bacillus

subtilis. PLoS Genet. 2020 Dec 14;16(12):e1009246. doi: 10.1371/journal.pgen.1009246. PMID: 33315869; PMCID: PMC7769602.
19. Qin Y, Faheem A, Hu Y. A spore-based portable kit for on-site detection of fluoride ions. J Hazard Mater. 2021 Oct 5;419:126467. doi: 10.1016/j.jhazmat.2021.126467. Epub 2021 Jun 24. PMID: 34182423.
20. Cabeen MT, Jacobs-Wagner C. Bacterial cell shape. Nat Rev Microbiol. 2005 Aug;3(8):601-10. doi: 10.1038/nrmicro1205. PMID: 16012516.
21. Wang Q, Xiao L, He Q, Liu S, Zhang J, Li Y, Zhang Z, Nie F, Guo Y, Zhang L. Comparison of hemolytic activity of tentacle-only extract from jellyfish Cyanea capillata in diluted whole blood and erythrocyte suspension: diluted whole blood is a valid test system for hemolysis study. Exp Toxicol Pathol. 2012 Nov;64(7-8):831-5. doi: 10.1016/j.etp.2011.03.003. Epub 2011 Apr 6. PMID: 21474292.
22. Dubay MM, Acres J, Riekeles M, Nadeau JL. Recent advances in experimental design and data analysis to characterize prokaryotic motility. J Microbiol Methods. 2023 Jan;204:106658. doi: 10.1016/j.mimet.2022.106658. Epub 2022 Dec 15. PMID: 36529156.
23. Wang C, Zhang Y, Luo H, Zhang H, Li W, Zhang WX, Yang J. Iron-Based Nanocatalysts for Electrochemical Nitrate Reduction. Small Methods. 2022 Oct;6(10):e2200790. doi: 10.1002/smtd.202200790. Epub 2022 Sep 14. PMID: 36103612.
24. Hu CY, Cheng HY, Yao XM, Li LZ, Liu HW, Guo WQ, Yan LS, Fu JL. Biodegradation and decolorization of methyl red by *Aspergillus versicolor* LH1. Prep Biochem Biotechnol. 2021;51(7):642-649. doi: 10.1080/10826068.2020.1848868. Epub 2020 Nov 23. PMID: 33226883.
25. Xu D, Wu L, Yao H, Zhao L. Catalase-like nanozymes: Classification, Catalytic Mechanisms, and Their Applications. Small. 2022 Sep;18(37):e2203400. doi: 10.1002/smll.202203400. Epub 2022 Aug 15. PMID: 35971168.
26. Pawlik A, Stefanek S, Janusz G. Properties, Physiological Functions and Involvement of Basidiomycetous Alcohol Oxidase in Wood Degradation. Int J Mol Sci. 2022 Nov 9;23(22):13808. doi: 10.3390/ijms232213808. PMID: 36430286; PMCID: PMC9699415.
27. Cordaro JT, Sellers W. Blood coagulation test for citrate utilization. Appl Microbiol. 1968 Jan;16(1):168-9. doi: 10.1128/am.16.1.168-169.1968. PMID: 5636461; PMCID: PMC547351.
28. Krajang M, Malairuang K, Sukna J, Rattanapradit K, Chamsart S. Single-step ethanol production from raw cassava starch using a combination of raw starch hydrolysis and fermentation, scale-up from 5-L laboratory and 200-L pilot plant to 3000-L industrial fermenters. Biotechnol Biofuels. 2021 Mar 16;14(1):68. doi: 10.1186/s13068-021-01903-3. PMID: 33726825; PMCID: PMC7962325.
29. Kerwin BA. Polysorbates 20 and 80 used in the formulation of protein biotherapeutics: structure and degradation pathways. J Pharm Sci. 2008 Aug;97(8):2924-35. doi: 10.1002/jps.21190. PMID: 17973307.
30. Trueba FJ, Neijssel OM, Woldringh CL. Generality of the growth kinetics of the average individual cell in different bacterial populations. J Bacteriol. 1982 Jun;150(3):1048-55. doi: 10.1128/jb.150.3.1048-1055.1982. PMID: 6804435; PMCID: PMC216321.
31. McCrea KW, Xie J, LaCross N, Patel M, Mukundan D, Murphy TF, Marrs CF, Gilsdorf JR. Relationships of non-typeable Haemophilus influenzae strains to hemolytic and nonhemolytic Haemophilus haemolyticus strains. J Clin Microbiol. 2008 Feb;46(2):406-16. doi: 10.1128/JCM.01832-07. Epub 2007 Nov 26. PMID: 18039799; PMCID: PMC2238123.
32. Jogawat A, Vadassery J, Verma N, Oelmüller R, Dua M, Nevo E, Johri AK. PiHOG1, a stress regulator MAP kinase from the root endophyte fungus Piriformospora indica, confers salinity stress tolerance in rice plants. Sci Rep. 2016 Nov 16;6:36765. doi: 10.1038/srep36765. PMID: 27849025; PMCID: PMC5111105.
33. Barry AL, Feeney KL. Two quick methods for the Voges-Proskauer test. Appl Microbiol. 1967 Sep;15(5):1138-41. doi: 10.1128/am.15.5.1138-1141.1967. PMID: 4865027; PMCID: PMC547154.
34. Wang J, Su Y, Jia F, Jin H. Characterization of casein hydrolysates derived from enzymatic hydrolysis. Chem Cent J. 2013 Apr 4;7(1):62. doi: 10.1186/1752-153X-7-62. PMID: 23556455; PMCID: PMC3626679.
35. de Bie TH, Witkamp RF, Balvers MG, Jongsma MA. Effects of γ-aminobutyric acid supplementation on glucose control in adults with prediabetes: A double-blind, randomized, placebo-controlled trial. Am J Clin Nutr. 2023 Sep;118(3):708-719. doi: 10.1016/j.ajcnut.2023.07.017. Epub 2023 Jul 24. PMID: 37495019.
36. Endoh R, Horiyama M, Ohkuma M. D-Fructose Assimilation and Fermentation by Yeasts Belonging to Saccharomycetes: Rediscovery of Universal Phenotypes and Elucidation of Fructophilic Behaviors in *Ambrosiozyma platypodis* and *Cyberlindnera americana*. Microorganisms. 2021 Apr 5;9(4):758. doi: 10.3390/microorganisms9040758. PMID: 33916327; PMCID: PMC8065679.
37. Lu Z, Guo W, Liu C. Isolation, identification and characterization of novel Bacillus subtilis. J Vet Med Sci. 2018 Mar 24;80(3):427-433. doi: 10.1292/jvms.16-0572. Epub 2018 Jan 23. PMID: 29367516; PMCID: PMC5880821.
38. Zhao Y, Meng K, Fu J, Xu S, Cai G, Meng G, Nielsen J, Liu Z, Zhang Y. Protein engineering of invertase for enhancing yeast dough fermentation under high-sucrose conditions. Folia Microbiol (Praha). 2023 Apr;68(2):207-217. doi: 10.1007/s12223-022-01006-y. Epub 2022 Oct 6. PMID: 36201138.

39. Irschik H, Gerth K, Höfle G, Kohl W, Reichenbach H. The myxopyronins, new inhibitors of bacterial RNA synthesis from Myxococcus fulvus (Myxobacterales). J Antibiot (Tokyo). 1983 Dec;36(12):1651-8. doi: 10.7164/antibiotics.36.1651. PMID: 6420386.
40. Wiegand I, Hilpert K, Hancock RE. Agar and broth dilution methods to determine the minimal inhibitory concentration (MIC) of antimicrobial substances. Nat Protoc. 2008;3(2):163-75. doi: 10.1038/nprot.2007.521. PMID: 18274517.
41. Balouiri M, Sadiki M, Ibnsouda SK. Methods for in vitro evaluating antimicrobial activity: A review. J Pharm Anal. 2016 Apr;6(2):71-79. doi: 10.1016/j.jpha.2015.11.005. Epub 2015 Dec 2. PMID: 29403965; PMCID: PMC5762448.
42. Dell'Anno A, Fabiano M, Duineveld GCA, Kok A, Danovaro R. Nucleic acid (DNA, RNA) quantification and RNA/DNA ratio determination in marine sediments: comparison of spectrophotometric, fluorometric, and high-performance liquid chromatography methods and estimation of detrital DNA. Appl Environ Microbiol. 1998 Sep;64(9):3238-45. doi: 10.1128/AEM.64.9.3238-3245.1998. PMID: 9726866; PMCID: PMC106716.
43. Simonian MH. Spectrophotometric determination of protein concentration. Curr Protoc Cell Biol. 2002 Aug;Appendix 3:Appendix 3B. doi: 10.1002/0471143030.cba03bs15. PMID: 18228395.
44. Rox K, Becker T, Schiefer A, Grosse M, Ehrens A, Jansen R, Aden T, Kehraus S, König GM, Krome AK, Hübner MP, Wagner KG, Stadler M, Pfarr K, Hoerauf A. Pharmacokinetics and Pharmacodynamics (PK/PD) of Corallopyronin A against Methicillin-Resistant *Staphylococcus aureus*. Pharmaceutics. 2022 Dec 30;15(1):131. doi: 10.3390/pharmaceutics15010131. PMID: 36678760; PMCID: PMC9860980.
45. Xu J, Jin H, Zhu H, Zheng M, Wang B, Liu C, Chen M, Zhou L, Zhao W, Fu L, Lu Y. Oral bioavailability of rifampicin, isoniazid, ethambutol, and pyrazinamide in a 4-drug fixed-dose combination compared with the separate formulations in healthy Chinese male volunteers. Clin Ther. 2013 Feb;35(2):161-8. doi: 10.1016/j.clinthera.2013.01.003. PMID: 23410999.
46. Utku Türk EG, Jannuzzi AT, Alpertunga B. Determination of the Phototoxicity Potential of Commercially Available Tattoo Inks Using the 3T3-neutral Red Uptake Phototoxicity Test. Turk J Pharm Sci. 2022 Feb 28;19(1):70-75. doi: 10.4274/tjps.galenos.2021.86344. PMID: 35227052; PMCID: PMC8892553.
47. Thomas DN, Wills JW, Tracey H, Baldwin SJ, Burman M, Williams AN, Harte DSG, Buckley RA, Lynch AM. Ames Test study designs for nitrosamine mutagenicity testing: qualitative and quantitative analysis of key assay parameters. Mutagenesis. 2023 Dec 19:gead033. doi: 10.1093/mutage/gead033. Epub ahead of print. PMID: 38112628.
48. Zhang, YY., Huang, YF., Liang, J. et al. Improved up-and-down procedure for acute toxicity measurement with reliable LD50 verified by typical toxic alkaloids and modified Karber method. *BMC Pharmacol Toxicol* 23, 3 (2022). https://doi.org/10.1186/s40360-021-00541-7.
49. Heuser E, Becker K, Idelevich EA. Bactericidal Activity of Sodium Bituminosulfonate against *Staphylococcus aureus*. Antibiotics (Basel). 2022 Jul 5;11(7):896. doi: 10.3390/antibiotics11070896. PMID: 35884150; PMCID: PMC9311858.
50. Irschik H, Gerth K, Kemmer T, Steinmetz H, Reichenbach H. The myxovalargins are new peptide antibiotics from Myxococcus fulvus (Myxobacterales). I. Cultivation, isolation, and some chemical and biological properties. J Antibiot (Tokyo). 1983 Jan;36(1):6-12. doi: 10.7164/antibiotics.36.6. PMID: 6432761.
51. Glaus F, Dedić D, Tare P, Nagaraja V, Rodrigues L, Aínsa JA, Kunze J, Schneider G, Hartkoorn RC, Cole ST, Altmann KH. Total Synthesis of Ripostatin B and Structure-Activity Relationship Studies on Ripostatin Analogs. J Org Chem. 2018 Jul 6;83(13):7150-7172. doi: 10.1021/acs.joc.8b00193. Epub 2018 Mar 29. PMID: 29542926.
52. Dennison TJ, Smith JC, Badhan RKS, Mohammed AR. Formulation and Bioequivalence Testing of Fixed-Dose Combination Orally Disintegrating Tablets for the Treatment of Tuberculosis in the Paediatric Population. J Pharm Sci. 2020 Oct;109(10):3105-3113. doi: 10.1016/j.xphs.2020.07.016. Epub 2020 Jul 22. PMID: 32710905.
53. Alghamdi WA, Al-Shaer MH, Peloquin CA. Protein Binding of First-Line Antituberculosis Drugs. Antimicrob Agents Chemother. 2018 Jun 26;62(7):e00641-18. doi: 10.1128/AAC.00641-18. PMID: 29735566; PMCID: PMC6021678.